Highly Integrated, Very High Gain 20 Watt X-Band SSPA in GaN Technology

Przemyslaw KANT, Jerzy Julian MICHALSKI

Dept. of Research and Development, Pomeranian Science and Technology Park,
Al. Zwyciestwa 96/98, 81-451 Gdynia, Poland

przemyslaw.kant@spaceforest.pl, jerzy.michalski@spaceforest.pl

Submitted February 10, 2021 / Accepted December 9, 2021

Abstract. *This paper shows design and development of a highly integrated solid state power amplifier (SSPA) operating in X-Band. The last amplifying stage is realized in GaN technology. To the best of authors' knowledge, for the first time in the high power amplifier, the vertical orientation of the last amplification stage was used, which allowed to significantly minimize the footprint of the device while maintaining high output power and PAE. The device includes full digital control over the entire RF chain using a custom BIAS ASIC controlled via SPI interface, assuring high flexibility and stability of the SSPA. The SSPA operates in a wide frequency range of 8.025–8.4 GHz with 20 watt output power at input power range of –20 dBm to 0 dBm and power added efficiency (PAE) reaching up to 35%. Although the main application of presented SSPA is earth observation (EO) it can be used in ground segment, e.g. for radar application as well.*

Keywords

Microwave amplifier, solid state power amplifier, SSPA, GaN technology

1. Introduction

A typical satellite consists of a hundreds of RF or microwave devices, allowing proper receiving, processing and transmitting of the data. Among different types of on-board equipment, some of the most critical components are transmitters including power amplifiers. The transmitters are used for multiple purposes, such as sending telemetry data, measurement instruments data or relaying received data. In most of cases the transmission is made from the satellite towards the Earth. A traditional satellite includes a number of typically dual-redundant transmitters operating at different frequencies and at different power levels. The power level depends on the frequency, orbit and the bandwidth of the transmitted signal, determining the parameters of the high power amplifier included in the transmitter. A classical approach to generate high power RF/microwave signals on board of a satellite was based on using traveling-wave tube amplifiers (TWTA). In case of a TWTA, the RF/microwave power is increased by absorbing power from a beam of electrons passing through a tube between electron gun and collector. The TWTAs are still widely used due to a number of benefits, such as ability to reach output power levels in the area of hundred watts - kilowatts, high power added efficiency (PAE) in the area of 60% at X-Band and others. Although very powerful, the TWTAs also have some drawbacks, among which the highest are necessity to use very high voltage power supplies (in the range of kV), large mass and size and high cost, especially important from the perspective of the emerging "new space" market, requiring low cost at high reliability [1], [2]. An alternative to TWTA technology is use of solid-state power amplifiers (SSPAs). For many years, the high frequency SSPAs based on GaAs devices, allowing to reach typical output power levels of tens of watts were used. The limitations of GaAs technology, such as rather low electron bandgap, low breakdown field and low thermal conductivity limited for many years the maximum output power level and the PAE of the HPAs [2]. With emerging of GaN technology, manufacturing of highly efficient high power amplifiers became possible. Thanks to a high thermal conductivity of GaN, high breakdown voltages and a much wider electron bandgap, the GaN-based SSPA can provide higher output power (hundreds of watts per single component) and higher power efficiency exceeding 50% at X Band. Additional benefits for space equipment involve their inherent radiation hardness and tolerances of higher bus-voltages and operational temperatures. With use of GaN devices the HPA-based SSPA can bring the following benefits to the design in comparison to the TWTA-based transmitter such as smaller volume and footprint, lower cost, use of voltages in a range of 28–100 V and overall higher reliability [1], [2]. Although the GaN-based SSPAs are behind TWTA technology in some aspects, such as lower output power (typically tens-hundreds of watts), slightly lower max. PAE, lower maximal frequency (current devices operating below 40 GHz), necessity to use thermal stabilization / compensation and necessity to dissi-

DOI: 10.13164/re.2022.0077

Ref.	**Cent. freq.** [MHz]	**BW** [MHz]	**Out. pow.** [dBm]	**Gain** [dB]	**PAE** [%]	**Dim.** [L×W×H mm^3]
[3]	8450	100	41.75	38	32.5	150×120×62
ESA SPOT-5 [3]	8153–8365	50	43.4	-	24.2	-
ESA SPOT, Helios, Skynet [3]	X-Band	-	42.3	-	24.4	-
NASA MER [3]	X-Band	-	42.3	-	28.8	-
[4]	7200	-	42.3/44	-	30/37.5	separate modules
[5]	8200	200	41.95	38	21	180×140×50
[6]	8425	60	42.3	41.3	28.8	171×133×44.5
[7]	9900	900	50 (in pulse)	47	28.2	-
[8]	9850	1000	53.2(in pulse)	41.4–43.1	36.5–43.6	-
[10]	10640	150	40	20*	40	50×60×40
This work [9]	8212.5	375	43	64	31/26.5**	188×35×96

* Amplifier module including upconverter.

** First value - typical PAE (up to 35% for some frequencies) of the SSPA without the DC/DC unit. The second value - PAE including a typical DC/DC converter efficiency

Tab. 1. Comparison of the developed SSPA with other solutions at similar output power and frequency.

pate heat from point-sources, the GaN-based SSPAs meets with great interest from the space industry. This was the main motivation for the work presented in this paper. The modern cost-effective GaN components allow to achieve high output power level at power added efficiency exceeding 50% at X-Band. With these benefits, use of this technology for low cost, new space large scale satellite constellations becomes an obvious choice. The main use case for such amplifiers / transmitters is data transmission from space to Earth from Earth Observation Constellation satellites. A typical operation frequency band for such transmitters is 7.9–8.4 GHz. The presented amplifier should operate in the frequency range of 8.025–8.4 GHz, allowing use with a dedicated modulator providing wideband PSK signal with up to 256 symbols. The amplifier, modulator and a control unit should be integrated into a single, highly integrated transmitter, showing high efficiency, high transmission speed and low footprint and mass of the entire assembly, offering many advantages for the new space market over the existing transmitters. As the total PAE of the SSPA is significantly influenced by the insertion losses of the output structures (output isolator, RF connectors, output waveguide/cavity filter, output biasing and matching structures etc.) and by dissipated power in other RF and DC components included in the SSPA, the total efficiency of the entire SSPA is typically significantly lower in comparison to the PAE of the power stage alone. Still, PAE, output power level and power gain of the power amplifier are the most critical parameters of the HPA to characterize the performance of the entire SSPA. There have been designed SSPAs with efficiency exceeding 30%, as can be found in Tab. 1, summarizing some of the recently developed SSPAs for space applications. The currently developed SSPA shows advantages in the total operational bandwidth, very high gain, full digital control over all parameters thanks to use of a BIAS ASIC and the smallest footprint.

One of the most critical requirements for the spaceborne SSPA is the output power stability versus change of temperature, which in a typical case of an EO satellite, is in a range of −35°C to +65°C. The necessity to compensate the output power in a wide temperature range comes from the operation environment, which requires operation during a direct exposure of the satellite to sun radiation (very high outer temperature) and during operation in the shadow of the Earth (very low temperature). Although satellites include temperature control systems, the SSPA needs to keep the same output power level in a wide range of temperatures. In order to stabilize the output power level, ALC (automatic level control) has also been introduced to the SSPA. The ALC circuit sets the gate voltages of the variable gain amplifiers, thus regulating the gain of these amplifiers, to keep the output power level stable at different environmental conditions. Typical input parameters for the ALC algorithm are voltage from the power detector and voltage from the temperature sensors. The ALC also allows to control the total gain of the SSPA at different input power levels from the range of –20 dBm to 0 dBm. This wide power level is a typical output power range of the modulator providing the input signal for the SSPA. The ALC, along with other parts of the SSPA will be described in detail in the following sections. The next section shows basic assumptions and the design of the SSPA. In the following section experimental verification of the amplifier is presented and described in detail. The last section concludes the paper.

2. Design of the SSPA

The designed SSPA needs to meet 20 W of output power requirement in the 8.025–8.4 GHz frequency band. In a typical case, contact area between the SSPA and the baseplate of the satellite is maximized in order to minimize the thermal resistance between the components generating most of the heat (mainly HPA) and the baseplate / TIM (Thermal Interface Material). Such mounting, although beneficial from thermal point of view, is not optimal as vertical mount of the device allows to design a much more compact integrated transmitter including the SSPA slice, modulator slice and the Customer Interface Unit slice including DC/DC and all the equipment handling TM/TC (Telemetry/Telecommand) communication. A conceptual depiction of the device can be found in Fig. 1.

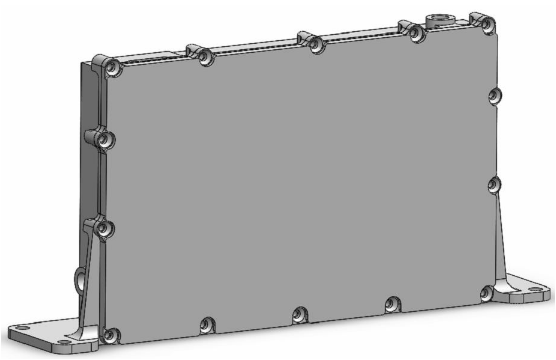

Fig. 1. Depiction of the vertically mounted SSPA.

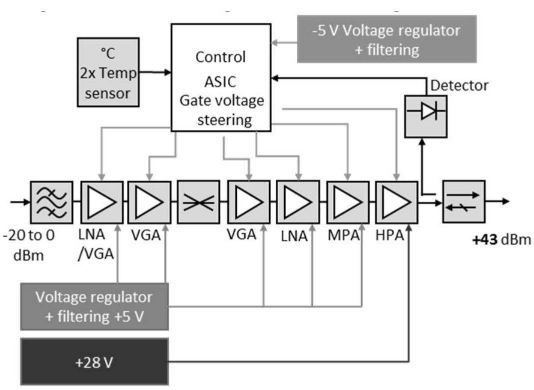

Fig. 2. Block diagram of the +43 dBm SSPA.

Having the mounting method fixed, the block diagram of the SSPA has been defined. As the device needs to assure more than 63 dB of the total gain at a nominal temperature (25°C) in order to reach +43 dBm output at –20 dBm input, the structure of the RF chain needs to include multiple elements assuring the required gain and output power levels. The actual gain required to generate 20 watt output is higher by more than 10 dB due to insertion losses of multiple passive structures, microstrip paths, compression and thermal drifts of the devices. The goal for design of this device was to use off-the-shelf, cost-effective packaged devices, allowing easy transition to bare die MMIC design in the EQM (Engineering Qualified Model) and the FM (Flight Model) projects. The block diagram of the device including the RF path, control circuits and the DC circuits and allowing to achieve the required performance can be found in Fig. 2. The DC circuits include voltage regulators for positive and negative voltage. The negative voltage regulator, providing stable voltage for the the BIAS ASIC, was based in this approach on an integrated component including low internal noise from Texas Instruments (TPS7A3001), which in the target device should be replaced by a discrete design-based voltage regulator or a rad-tolerant component. The positive voltage regulator was based on discrete design of a linear regulator based on a low noise operational amplifier (Analog OP27), opening or closing channel of the p-channel MOSFET transistor (Infineon IPD042P03) depending on the difference between the actual output voltage of the regulator and the voltage of a stable voltage reference. In order to assure high stability of the regulated voltage, temperature stable 2.5 V voltage reference (Linear LT1009) and thermally stable resistors sampling and dividing the output voltage needed to be included in the design.

The discrete design allows to have a higher control over radiation effects for lower grade components. By using intense RC filtering in the main line of the regulator, influence of SET (Single Event Transients) pulses, which are caused by heavy ions hitting on-chip structures and causing short-term short circuit, typically to rail, the transient response of the regulators can become much smoother and milder, protecting the electronics from overvoltage (drain) or overcurrent (gates). Also appropriate choice of active components is necessary to assure resistance of the regulators to ionization radiation doses. The most critical components are integrated circuits, such as operational amplifier and voltage reference and MOSFET transistors. The choice of the MOSFET transistors for new space equipment is especially difficult and requires careful choice of components in respect to TID (Total Ionization Dose) and SEB (Single Event Burnout) and SEGR (Single Event Gate Rapture) performance.

The voltages made available for the SSPA are +28 V for the high power stage, +6 V for the low power stages and –6 V for the control circuit and gates of the GaAs and GaN amplifiers. As the lower voltages are only roughly regulated, additional regulation and filtering needs to be added on the SSPA level (regulation to +5.5 V for the positive and to –5 V for negative voltage using both discrete and integrated linear voltage regulators). The 28 V is already well regulated so only additional filtering has been added to the SSPA PCB. The control circuit includes a custom bias ASIC (application-specific integrated circuit) designed and manufactured by the project partner. The ASIC includes 8 DAC (digital-analog converter) outputs and 4 differential ADC (analog-digital converter) inputs. Additional inputs are used to read out device parameters such as board temperature (2 diodes used as temperature sensors included in the SSPA) and output power level using detector diode circuit based on a Schottky detector diode. The diode is used to sense a part of the output signal coupled using a directional coupler. Additional features include, use of drain current controllers (each independently stabilizing drain current for low power devices), functions allowing to turn on and off certain amplifiers included in the SSPA and implementation of the ALC - Automatic Level Control. The ALC is based on information from the temperature sensors (information from general purpose Si diodes based on temperature change of forward voltage), output power sensor (DC voltage from a Schottky-diode detector sampling output power via a directional coupler) and look-up tables (LUTs) including characteristics of the VGAs (variable gain amplifiers). Basing on the input information (typical examples of the LUT input data in Fig. 3) the ALC algorithm (PID regulator included in the bias ASIC) calculates gate voltage values for the VGAs included in the RF path in order to compensate the thermal drifts of the amplifiers assuring stabilization of the output signal level. The control over bias ASIC is being done using SPI serial protocol

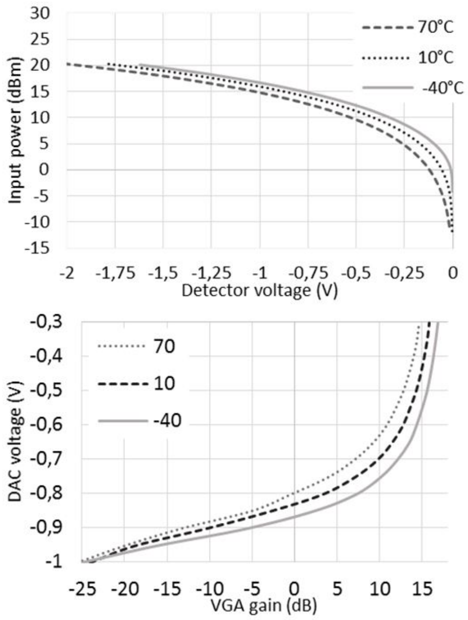

Fig. 3. Typical data gathered in bias ASICs LUTs allowing to calculate the output power level basing on the detector voltage (top figure) and the required gate voltage for the VGA to set the right gain level (bottom figure) at different temperatures.

connecting the control ASIC with a higher level control device performing Telemetry/Telecommand functions. Use of the custom, high performance and space-qualified bias ASIC allows to achieve full digital control over the amplifier, which allows to reconfigure the SSPA even during its operation (change of output level, gain, compression etc.).

The RF path includes in total 6 amplification stages, which can be divided into 3 groups:

- Low power stages - UMS CHA3024-QGG - the device includes 4 low noise amplifiers including VGA (Variable Gain Amplifier) functions. The components allows to set gain/attentuation in a range of 30 dB by changing 2 dedicated gate voltages. A typical max. gain value of a single stage is between 12–15 dB, depending on the temperature. The distributed LNAs/VGAs are manufactured in 0.15 µm GaAs pHEMT process. The first stage is set to low NF (noise figure), 2nd and 3rd stages are used for gain compensations (based on ALC algorithm response) and the 4th stage is set for high linearity (high current), driving the Medium Power Amplifier,

- Medium Power Amplifier - Qorvo TGA2701-SM - GaAs amplifier capable of generating high output (P1dB above 2 watts) and including high gain (18 dB). The amplifier is manufactured in 0.25 µm GaAs pHEMT process. The MPA gate voltage of the MPA is kept on a constant level,

- High Power Amplifier - CREE CGHV96050F - high PAE (theoretically exceeding 50%), high power gain (up to 12 dB) GaN HEMT on SiC amplifier including internal pre-matching structures. The device is included on a Molybdenum-Copper carrier to reduce the thermal resistance to the baseplate. The nominal drain voltage for this component is 40 V (about 50 Watt output), however in the currently described SSPA the drain voltage is limited to 28 V due to limitations of the typical voltage bus on small EO satellites and a lower required output power.

The amplifier stages are based on off-the-shelf packaged components with additional planar matching (MPA, HPA) and biasing structures (HPA) included on a 4-layer PCB. The PCB is based on a low loss Megtron-family material from Panasonic. The PCB is gold-plated. To assure low operating temperatures of components, the PCB includes multiple ground vias and mounting screws for improved heat transfer, especially in proximity of the MPA and HPA. To further improve the heat transfer between the active components and the chassis, high thermal conductivity thermal paste was used below the MPA area of the multilayer PCB and between the HPA and the chassis. The target design is to be based on bare dies only. Other structures included in the RF path are planar filters, passive equalizer circuit and output structures such as output coupler including a detector circuit and output isolator assuring good matching of the SSPA towards the output bandpass filter and the antenna. The filters are based on 3rd order interdigital bandpass structures reducing gain outside the required frequency band. A typical in-band insertion loss of the filter is 0.6 dB. Other circuit is the equalizer, which was based on four open stubs connected via resistors to the through RF microstrip lines. Change of slope can be achieved by changing lengths of the open stubs and by changing resistor values. The output structures of the SSPA include an output directional coupler based on coupled lines with coupling factor of –25 dB and an output isolator from NOVA showing a relatively high value of –0.4 dB of in-band insertion loss and 25 dB of isolation. The output structures significantly influence the overall PAE of the device.

The PCB including all the devices has been attached to an aluminum chassis designed in a way allowing to minimize the thermal resistance between active components and the satellite baseplate for the vertical mounting, especially for the HPA. This is important in context of high reliability, which needs to be assured also for new space components, designed to survive up to 7 years in a low earth orbit (LEO). By using a high thermal conductivity Aluminum alloy, optimizing the area of the foot (plane of contact with the satellite baseplate) and location of the heat generating components as close as possible to the baseplane of the satellite, it was possible to achieve junction temperatures for all active elements below the values required by the ECSS (European Commission for Space Standardization) requirements, which are 115°C for GaAs pHEMT junction (125°C allowed conditionally) and 160°C for GaN HEMT transistors. Due to a very high amount of gain in a compact chassis it is crucial to assure highest possible isolation between different amplifier stages. To assure this, a number of grounded vias were added, which together with aluminum walls included in the top lid of the SSPA form cavities, which minimize interstage couplings between the amplifiers. To make the mechanical design independent of PCB height tolerances, conductive rubber gaskets were added into groves included in the cavity walls. The external interfaces include two SMA screw-on type female receptacles with appropriate pins as RF input and output. DC voltages are connected via screwed-in feedthrough filters for additional voltage filtering. The SPI connection is via micro 15-line D-Sub connector. A visualization of the entire SSPA including the PCB, components, chassis and section through the top lid showing the cavity walls, can be found in Fig. 4. The full model has been manufactured and tested. The initial verification results were published by authors in [9].

3. SSPA Performance

The nominal operating point (NOP) of the SSPA is –10 dBm input and 20 watt (+43 dBm) output. Wideband measurement of the input reflection and total gain at –10 dBm input and 20 watt output can be seen in Fig. 6. For the worst case scenario (–20 dBm input, 20 watt output), the in-band ripple was at a level of 0.3 dB, which can be seen in Fig. 7. The in-band ripple tends to increase at higher power levels due to increased compression at the edges of the frequency range. This was caused mainly by the necessity to manually tune the HPA matching due to a problem with an invalid non-linear model from the component manufacturer.

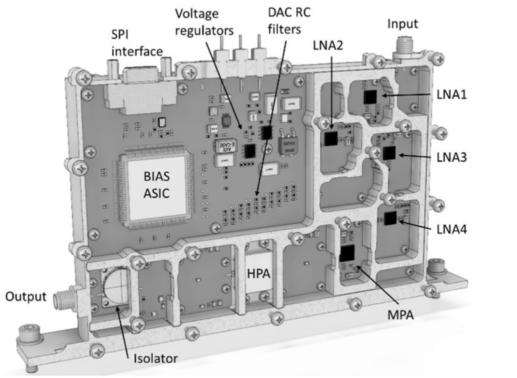

Fig. 4. Model of the SSPA including all components, PCB housing and section of the lid including the cavity walls.

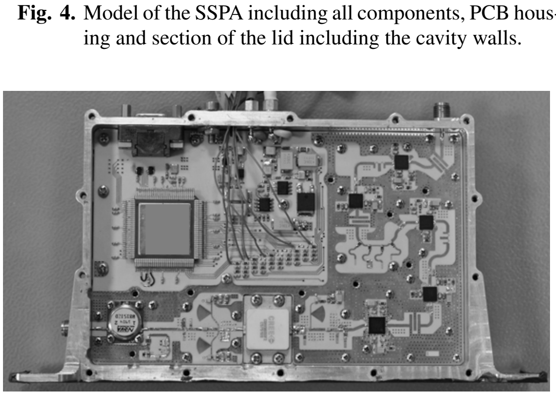

Fig. 5. Fully assembled X-Band SSPA including the chassis, PCB and components. Additional wires added to monitor gate voltages levels of the active components.

The increased compression at the edges of the band is especially visible in Fig. 8 showing output power in a function of the input power for configuration set by the bias ASIC. Figure 9 shows the corresponding PAE of the entire device including losses of the output isolator and the voltage regulators. The increased compression at the band edges influences significantly the harmonics levels. Figure 10 shows the 2nd harmonics levels for different in-band frequencies at 20 W output. At higher power levels the harmonics levels at the edges of the frequency range increase due to increased compression. As described, this phenomenon is caused due to a non-optimal tuning of the output power stage.

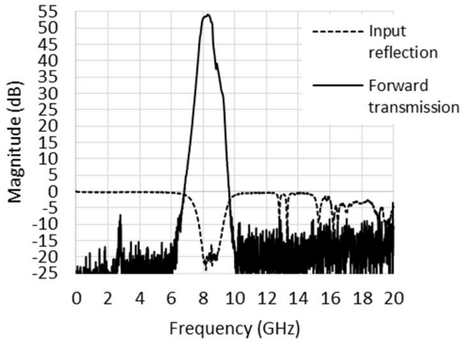

Fig. 6. Total gain and the input reflection scattering parameter of the X-Band SSPA at –10 dBm input.

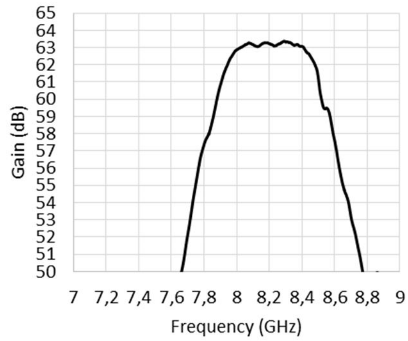

Fig. 7. The close-up of the total transmission of the SSPA for –20 dBm input and 20 watt output configuration.

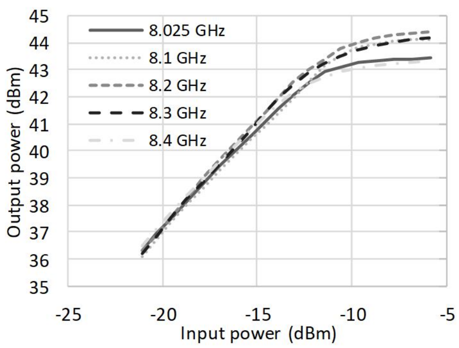

Fig. 8. Output power versus input power at different frequencies for a typical high output power configuration.

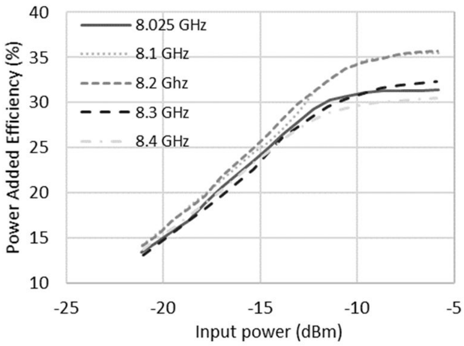

Fig. 9. PAE of the entire device including the output isolator versus input power level at different frequencies for a typical high output power configuration.

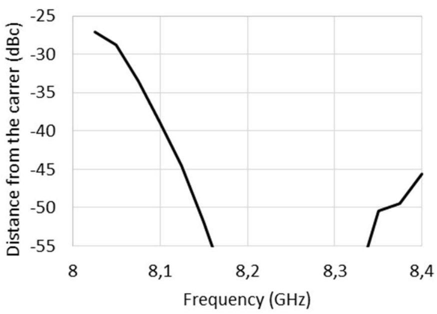

Fig. 10. 2nd harmonic levels for the corresponding in-band fundamental frequencies (8–8.4 GHz) at 20 W output.

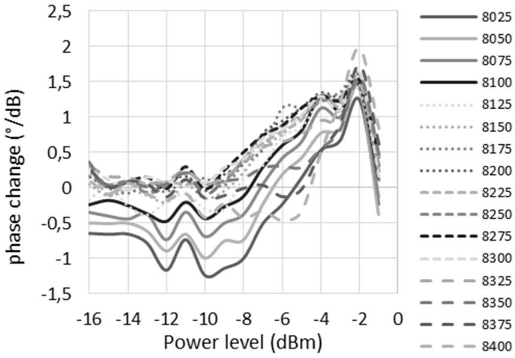

Fig. 11. AM/PM distortion measurement of the SSPA for 20 W output at 0 dBm input configuration.

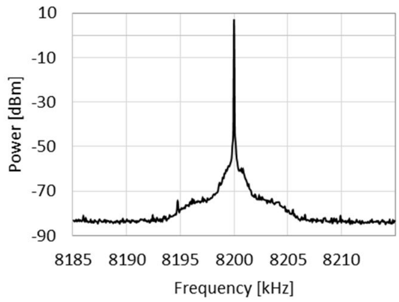

Fig. 12. Wideband spurious signals measurement showing lack of spurious signals other than from the measurement device. Measurement done at 20 W output including output attenuators (34 dB of attenuation added in total not included in the measurement).

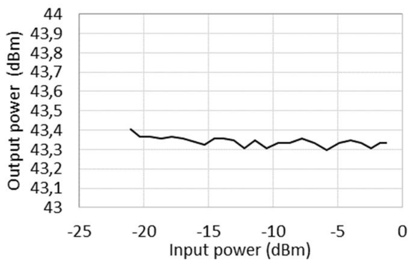

Fig. 13. Output power level of the SSPA during change of input power level at a constant temperature. Measurement done at 8.2 GHz.

One of the most critical parameters of the SSPA used with wideband signals including complex modulation schemes is the AM/PM distortion, which can be characterized as undesired phase variation (PM) caused by amplitude variations (AM). The AM-to-PM conversion is critical in systems where phase (angular) modulation is used, causing analog signal degradation or increased BER (Bit Error Rate) in digital communication systems.

In case of the presented SSPA the target PSK-type modulation should include up to 256 symbols, which results in AM/PM requirement of 2.5 deg/dB. The SSPA AM/PM measurement for the 0 dBm configuration with 20 W output can be seen in Fig. 11. It can be seen that the maximum value of the AM/PM distortion reaches 2 deg/dB, which is an acceptable value. Similar results were obtained for all other configurations of the SSPA. As a linearizer is to be used with the target SSPA, the AM/AM distortions are not that critical.

Another important parameter is spectrum purity at the output of the SSPA. The main sources of the spurious signals can be found in the DC/DC (especially the switching frequency) and in the bias ASIC, especially at the junction of digital and analog domains, which are the DACs steering the gates of the RF amplifiers. To limit the influence of the DC/DC, voltage regulators with significant RC filtering have been added, allowing to filter out the unwanted signals. In order to clean the DACs from the unwanted signals, 2nd order RC filters were also added to these output. As no current is flowing through gate lines, significant RC filtering has been added, allowing to get rid of the unwanted signals in the range starting from single kHz. As a result, the output spectrum of the SSPA is free from spurious signals, which can be seen in Fig. 12. This has a significant impact on the target BER during communication between the satellite and the ground station. As the SSPA needs to operate in an autonomous mode, i.e. it needs to be capable of compensating for drifts caused by change of the input power level and by change of the SSPA reference temperature, tests using ALC including the defined LUTs needed to be performed. The initial tests included investigation of the ALC algorithm during change of the input power level at a single frequency. This tests show if the LUTs for the detector and the VGAs at a constant temperature are defined properly. The performance of the ALC algorithm can be seen in Fig. 13. It can be seen that the output power is kept at a constant level for a wide range of input powers. The maximum deviation of the ALC algorithm was 0.070 dB for 20 dB of input power level variation.

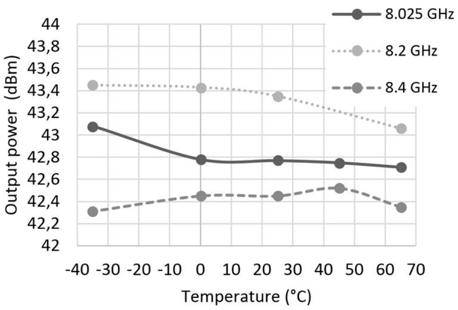

Fig. 14. ALC performance (output power level) at different frequencies in function of temperature. Data set (LUTs) prepared at 8.2 GHz.

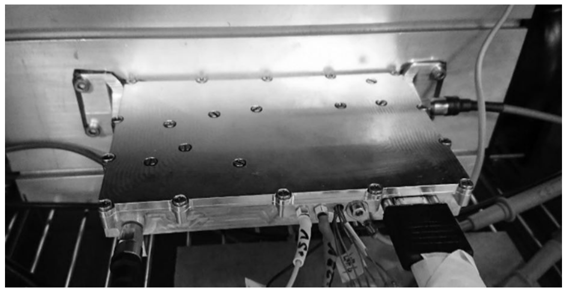

Fig. 15. Fully assembled X-Band SSPA during thermal tests.

After tests at a constant temperature, further tests of the ALC in autonomous mode at different temperatures were carried out. Figure 14 shows performance of the entire SSPA in fully autonomous mode at three different frequencies in the required temperature range. In order to define the thermal LUTs, characteristics of the amplifier, diode temperature sensor and diode detector were collected using dedicated test boards at 8.2 GHz. It can be seen in the figure that the output level drops at high temperatures, which was caused most probably by thermal drift of other components not characterized during definition of LUTs (DAC/ADC, output isolator etc.). This would not be the case if the entire SSPA would be used to gather characteristics necessary to form the LUTs. Still, the bias ASIC always indicated the right power level showing its proper operation. At 8.025 GHz and 8.4 GHz, LUTs for 8.2 GHz were used showing rather good stability, however with field for improvement. Figure 15 shows the fully integrated X-Band SSPA attached to the radiator during thermal tests. The final dimensions of the amplifier $188 \times 35 \times 96$ mm^3, making it a very compact design. The final weight including all components was 472 g, however the mass was not fully optimized in this breadboard.

4. Summary

The SSPA operating in X-band has been designed, manufactured and tested. The SSPA based on high efficiency GaN HPA is capable of reaching 20 watt output (up to +44.4 dBm) with average PAE of approx. 31% (up to 35%). The SSPA is able to generate the required output for the entire input power range, showing good in-band flatness and phase compression characteristics. The built-in ALC based on the custom bias ASIC worked well in all test conditions, however additional tuning of the ALC algorithm and LUTs would be necessary to further improve the overall performance of the amplifier. The SSPA has reached technology readiness level TRL 5, which corresponds to validation of critical functions of the amplifier/breadboard in the relevant environment. Further development up to EQM (Engineering Qualified Model - TRL 7 is planned. With use of a higher power gain and more reliable matched GaN MMIC power amplifier, the SSPA should be able to meet PAE levels close to 40% for the entire device.

Acknowledgments

This work was performed within ESA Contract No. 4000125300/18/NL/CBi. The authors wish to thank ESA and ESA employees, especially Dr. Vaclav Valenta for support provided during project implementation.

References

[1] LOHMEYER, W. Q., ANCIENTO, R. J., CAHOY, K. L., Communication satellite power amplifiers: current and future SSPA and TWTA technologies. *International Journal of Satellite Communications and Networking*, 2016, vol. 34, no. 1, p. 95–113. DOI: 10.1002/sat.1098

[2] COLANTONIO, P., GIANNINI, F., LIMITI E. *High Efficiency RF and Microwave Solid State Power Amplifiers*. West Sussex (United Kingdom): John Wiley & Sons, Ltd., 2009. ISBN: 9780470746547

[3] KOBAYASHI, Y., KAWASAKI, S. X-band, 15-W-class, highly efficient deep-space GaN SSPA for PROCYON mission. *IEEE Transactions on Aerospace and Electronic Systems*, 2016, vol. 52, no. 3, p. 1340–1351. DOI: 10.1109/TAES.2016.150207

[4] SHARMA, A., CHENG, S., LEHTONEN, et al. High efficiency 25 watt GaN X-band SSPA for deep space missions. In *IEEE Aerospace Conference*. Big Sky (MT, USA), 2017, p. 1–8. DOI: 10.1109/AERO.2017.7943723

[5] XIANFENG L., HAO G., YAXIANG J., et al. An X-band transmitter for small satellites. In *International Conference on Microwave and Millimeter Wave Technology (ICMMT)*. Guilin (China), 2007, p. 1–3. DOI: 10.1109/ICMMT.2007.381506

[6] BOGER, W., BURGESS, D., HONDA, R., et al. X-band, 17 watt, solid-state power amplifier for space applications. In *IEEE MTT-S International Microwave Symposium Digest*. Long Beach (CA, USA), 2005, p. 1379–1382. DOI: 10.1109/MWSYM.2005.1516940

[7] KIM, H. J., CHO, W. J., KWON J. H., et al. An X-band 100 W GaN HEMT power amplifier using a hybrid switching method for fast pulse switching. *Progress In Electromagnetics Research B*, 2017, vol. 78, p. 1–14. DOI: 10.2528/PIERB17030603

[8] CHEN H., JI X. F., JIANG L. J., et al. Design and implementation of an X-band pulsed solid-state power amplifier with high power and high efficiency using radial waveguide combiner. *Progress In Electromagnetics Research C*, 2011, vol. 21, p. 113–127. DOI: 10.2528/PIERC11030501

[9] KANT, P., MICHALSKI, J. J. Highly integrated X-band SSPA for new space market. In *International Microwave and Radar Conference (MIKON)*. Warsaw (Poland), 2020, p. 200–203. DOI: 10.23919/MIKON48703.2020.9253817

[10] ALIPARAST, P., NOGHANI, M. T., FARHADI, A., et al. Design of X-band SSPA based on GaN HEMT for telemetry subsystem of near-earth space missions. *AEU - International Journal of Electronics and Communications*, 2021, vol. 137, p. 1–11. DOI: 10.1016/j.aeue.2021.153781

About the Authors ...

Przemsylaw KANT was born in Olsztyn, Poland in 1986. He received the M.Sc. degree in High Frequency Engineering in 2012 from Karlsruhe Institute of Technology, Germany, and Technical University in Gdansk, Poland. He currently works as Head of Microwave Hardware section at SpaceForest Ltd., Gdynia, Poland. His major field is development of satellite electronic circuits, with main focus on ultra-low phase noise frequency generators and high power amplifiers.

Jerzy Julian MICHALSKI was born in 1974 in Rypin, Poland. He received the M.Sc. degree and Ph.D. in Electronic Engineering, from the Gdansk University of Technology in 1998 and National Research Institute in 2002, respectively. In 2013 he obtained D.Sc. higher doctorate degree (Habilitation) for development of novel methods of microwave filter tuning. He is actively serving non-profit organizations. In 2009–2012 he was Management Committee Member of European COST Action IC0803 RF / Microwave Communication Subsystems for Emerging Wireless Technologies (RFCSET). In 2013–2017 he was Management Committee Member of European COST Action IC1301 - Wireless Power Transmission for Sustainable Electronics (WiPE). In 2013–2019 he served as Secretary/Treasurer, at Polish Joint Chapter AP/MTT/AES (IEEE). Since 2012 he is Member of Microwave Section at Polish Academy of Science (PAN). He is the author of one book and co-author of two book chapters and the author/co-author of about 45 peer reviewed scientific papers.